

Title	Seasonal and diurnal patterns of soil respiration in an evergreen coniferous forest: Evidence from six years of observation with automatic chambers
Author(s)	Makita, Naoki; Kosugi, Yoshiko; Sakabe, Ayaka; Kanazawa, Akito; Ohkubo, Shinjiro; Tani, Makoto
Citation	PLOS ONE (2018), 13(2)
Issue Date	2018-02-12
URL	http://hdl.handle.net/2433/230574
Right	© 2018 Makita et al. This is an open access article distributed under the terms of the Creative Commons Attribution License, which permits unrestricted use, distribution, and reproduction in any medium, provided the original author and source are credited.
Type	Journal Article
Textversion	publisher

RESEARCH ARTICLE

Seasonal and diurnal patterns of soil respiration in an evergreen coniferous forest: Evidence from six years of observation with automatic chambers

Naoki Makita^{1,2*}, Yoshiko Kosugi², Ayaka Sakabe², Akito Kanazawa^{2,3}, Shinjiro Ohkubo^{2,4}, Makoto Tani^{2,5}

1 Faculty of Science, Shinshu University, Nagano, Japan, **2** Graduate School of Agriculture, Kyoto University, Kyoto, Japan, **3** Public Works Research Institute, Tsukuba, Japan, **4** NARO Hokkaido Agricultural Research Center, Hokkaido, Japan, **5** Department of Environments and Conservation, University of Human Environments, Aichi, Japan

* macky@shinshu-u.ac.jp



OPEN ACCESS

Citation: Makita N, Kosugi Y, Sakabe A, Kanazawa A, Ohkubo S, Tani M (2018) Seasonal and diurnal patterns of soil respiration in an evergreen coniferous forest: Evidence from six years of observation with automatic chambers. PLoS ONE 13(2): e0192622. <https://doi.org/10.1371/journal.pone.0192622>

Editor: Dafeng Hui, Tennessee State University, UNITED STATES

Received: August 26, 2017

Accepted: January 26, 2018

Published: February 12, 2018

Copyright: © 2018 Makita et al. This is an open access article distributed under the terms of the [Creative Commons Attribution License](https://creativecommons.org/licenses/by/4.0/), which permits unrestricted use, distribution, and reproduction in any medium, provided the original author and source are credited.

Data Availability Statement: All relevant data are within the paper and its Supporting Information files.

Funding: This work was supported by the Japanese Ministry of Education, Culture, Sports, Science, and Technology (Grants-in-Aid for Scientific Research (grant numbers 23221009, 15H03845, 15K18719)) from the Japan Society for the Promotion of Science (<http://www.jsps.go.jp/>)

Abstract

Soil respiration (R_s) plays a key role in the carbon balance of forest ecosystems. There is growing evidence that R_s is strongly correlated with canopy photosynthesis; however, how R_s is linked to aboveground attributes at various phenological stages, on the seasonal and diurnal scale, remains unclear. Using an automated closed dynamic chamber system, we assessed the seasonal and diurnal patterns of R_s in a temperate evergreen coniferous forest from 2005 to 2010. High-frequency R_s rates followed seasonal soil temperature patterns but the relationship showed strong hysteresis. Predictions of R_s based on a temperature-response model underestimated the observed values from June to July and overestimated those from August to September and from January to April. The observed R_s was higher in early summer than in late summer and autumn despite similar soil temperatures. At a diurnal scale, the R_s pattern showed a hysteresis loop with the soil temperature trend during the seasons of high biological activity (June to October). In July and August, R_s declined after the morning peak from 0800 to 1400 h, although soil temperatures continued to increase. During that period, figure-eight-shaped diurnal R_s patterns were observed, suggesting that a midday decline in root physiological activity may have occurred in early summer. In September and October, R_s was higher in the morning than in the night despite consistently high soil temperatures. We have characterised the magnitude and pattern of seasonal and diurnal R_s in an evergreen forest. We conclude that the temporal variability of R_s at high resolution is more related to seasons across the temperature dependence.

Introduction

Knowledge of soil carbon (C) dynamics is essential for understanding the C balance in terrestrial ecosystems [1]. Gross primary production (GPP) and soil respiration (R_s) are major CO_2 fluxes between the atmosphere and terrestrial ecosystems. R_s accounts for more than two-

and by the Coca-Cola Foundation (<http://www.coca-colacompany.com/>).

Competing interests: The authors have declared that no competing interests exist.

thirds of ecosystem respiration ($98 \pm 12 \text{ Pg CO}_2 \text{ yr}^{-1}$) [2]. Even a small change in the CO_2 release via R_s processes would have a significant effect on atmospheric CO_2 concentration and potentially affect climate change [3,4]. Therefore, R_s is likely to be an important determinant of ecosystem C balance under future climate change scenarios.

Forest R_s shows significant temporal variation and is affected by environmental factors that control the metabolism of root- and soil-living organisms. It is also affected by environmental conditions controlling gaseous diffusion and convection [5,6]. Among the environmental factors, soil temperature is the most important abiotic factor controlling R_s [7]. Over the past decade, automated systems for recording R_s have been developed, providing temporally dense datasets [8,9]. Manual systems effectively cover spatial variability; however, automated monitoring enables the analysis of temporal variations in R_s rates during conditions such as nighttime and rainfall when manual measurements are impracticable [9–11]. This high temporal resolution also makes it possible to observe the response of R_s to rapid temporal changes in environmental conditions effectively without the use of linear interpolation or models [12,13].

As the automated chamber method has developed, there is growing evidence that R_s is closely correlated with C flux from aboveground to belowground over time scales ranging from hours to days and months [14–16]. Data from automated chambers indicate that R_s rates correspond to changes in canopy photosynthesis and environmental parameters directly affecting leaf CO_2 gas exchange, such as photosynthetic photon flux density and vapor pressure deficit [13,14,17]. Consequently, annual variations in the observed R_s do not always coincide with model estimates based on soil environmental factors [18,19].

On the seasonal scale, it is becoming increasingly evident that temporal variations in forest C balance and C allocation have a strong phenological component [20,21]. Aboveground, leaf phenology is characterized by seasonal patterns of growth and senescence. A recent study highlighted critical feedbacks between variation in leaf phenology and ecosystem productivity [22]. The timing of leaf development in spring and leaf senescence and abscission in autumn indicates the variability in C balance and C allocation in the trees. On the other hand, belowground phenology is characterized by pulses of root production during periods conducive to plant growth [23]. For many species, a primary flush in root production occurs between late spring and summer [24,25]. When root proliferation occurs in the spring, the amount of respiring tissue increases with temperature-dependent CO_2 effluxes to maintain root and mycorrhizal growth [26–28]. In this case, root respiration should reflect a combination of seasonal root growth variations and temperature responses to specific respiration rates. Nevertheless, less is known about the phenological pattern of R_s , which may be further complicated as patterns change with soil temperature. Quantifying the seasonality of these R_s processes is useful for improving models of ecosystem productivity and global biogeochemistry [3,4].

Another advantage of the automated system is that it can evaluate diurnal scales. Recent studies using measurements with high temporal resolution have shown that R_s can vary during the day at a given soil temperature, causing a diurnal hysteresis in the temperature–respiration relationship [29–31]. Phase lags between the diurnal signals of soil temperature and R_s have been reported [28, 32], resulting from processes such as photosynthate supply, heat transport, and CO_2 diffusion [33,34]. The supply of substrate to roots and soil microbes is a critical determinant of variations in R_s [7,15] and accurate annual R_s budgets [19]. Nevertheless, the diurnal patterns of R_s rate for each season remain unclear [35]. A recent study showed that C transport rates vary seasonally and are affected by soil environmental conditions [36–38]. Plant phenology potentially affects diurnal rhythms of whole-tree physiology (e.g., assimilate supply) and growth in forest ecosystems, which can influence the semi-elliptical shapes of the R_s -soil temperature regression curves [39]. Therefore, in forests, we suggest that the differences in diurnal patterns of R_s may be due to seasonal variations.

The present study aimed to characterize seasonal and diurnal patterns of R_s in a temperate evergreen coniferous forest consisting primarily of *Chamaecyparis obtusa* (Japanese cypress). To this end, R_s was measured at 30-min intervals for 6 years by an automated closed dynamic chamber system. The present work builds on the study of Kosugi et al. [40], in which CO_2 gas exchange between the atmosphere and an evergreen coniferous forest was determined using eddy covariance flux data at the same study site as that of the present study. The authors reported that the temperature dependence of canopy photosynthesis decreased significantly in winter and that plant phenology must be considered to understand the seasonality of forest CO_2 exchange. Nevertheless, few studies have linked R_s patterns in evergreen forests to seasonal differences in phenology. We tested the hypothesis that R_s shows clear diurnal and seasonal changes beyond the semi-empirical model of the response of R_s to soil temperature factors in an evergreen forest. Furthermore, we tested the hypothesis that the diurnal pattern of R_s would be influenced by seasonality.

Materials and methods

Study site

The study was conducted in a temperate coniferous forest in Kiryu Experimental Watershed (35°N, 136°E; 190–255 m above sea level; 5.99 ha) located in Shiga Prefecture, central Japan. The region has a monsoon climate. The forest consists of 50-year-old Japanese cypress (*Chamaecyparis obtusa* Sieb. et Zucc.) planted in 1959. The mean tree height (diameter at breast height [DBH] > 5 cm) was 17.3 m based on the tree census in March 2011. The annual mean air temperature and precipitation between 2005 and 2010 at this site were 13.4°C and 1595 mm yr⁻¹, respectively (S1 Fig). This region has a distinct climate; it has cold winters with little snow and hot, humid summers with high rainfall owing to the significant effect of the Asian monsoon. The mean monthly air temperature was the highest in August (25.0°C) and the lowest in January (2.8°C). This area typically has snowfall on several days during a year, which melts within a few days. Rain occurs throughout the year, with two peaks in summer: the early summer *baiu* front season and the late summer typhoon season. Summer in western Japan is warm and humid with sufficient rain; however, occasional moderate drought conditions can occur (S1 Fig). The soil is classified as a Haplic Cambisol with sandy loam or loamy sand texture. The mean C/N ratio, pH, and electrical conductivity of the 0–5 cm mineral soil layer were 19.0, 5.9, and 4.9 mS/m, respectively [41].

The study forest is one of the Asia Flux sites. Micrometeorological and $\text{CO}_2/\text{H}_2\text{O}$ flux data were collected by the observation tower [40,42]. To compare the net ecosystem exchange estimated by the eddy covariance method, CO_2 and H_2O exchanges of leaves [40], manual soil CO_2 efflux [43], and soil CH_4 flux [41] were evaluated at this site. The average and standard deviation of annual GPP, ecosystem respiration, and net ecosystem exchange were 2044 ± 149 , 1555 ± 158 , and -490 ± 109 g C m⁻² yr⁻¹, respectively [40].

Measurement of R_s , soil environment, and GPP

Three measurement plots were established in the study area, separated from each other by ≥ 25 m. R_s was measured continuously with high temporal resolution at one point per plot at 30-min intervals from 2005 to 2010. Measurements were performed with an automated closed dynamic chamber system fitted with an infrared $\text{CO}_2/\text{H}_2\text{O}$ analyzer (Li-840; Li-cor, Lincoln, NE, USA). The system consisted of a permanently connected chamber (length 0.3 m, width 0.3 m, height 0.2 m) with an automatically controlled chamber lid. To minimize error in the CO_2 efflux measurements in closed dynamic chambers through pressure changes, the chambers were designed to provide sufficient volume for the steady pressure in the closed-

chamber. The soil collars were inserted tightly into the ground up to 5 cm in depth prior to the start of the sampling period and were sealed permanently to the chamber. Chamber opening and closing were controlled by an air compressor (FH-02; MEIJI, Japan). Switching between chambers was regulated by the air flow from solenoid valves (CKD USB3-6-3-E; CKD Corp., Japan) and AC/DC controller (SDM-CD16AC; Campbell Scientific, USA). To prevent shadow on the collar, all chamber material was consisted of transparent acrylic. When the chamber was closed, the air sample was dehydrated with a gas dryer to remove water vapor in the sample air and then circulated by a mass flow-controlled diaphragm pump (APN-085; Iwaki Pumps, Japan; DM-403ST-25; MFG. CO., LTD., Japan) through polyethylene tubes to the CO₂/H₂O analyzer. The flow rate using a mass flow controller (MPC0005; Yamatake, Japan) was 1.8 L min⁻¹. Because not all of the water vapor could be removed by the drying system (PD-50 T-48; Perma Pure, Toms Rivers, NJ, USA), its presence was corrected by using the H₂O concentration measured with the CO₂/H₂O analyzer. The time interval for each measurement was set to 180 s. To compensate for air disturbances caused by opening the chamber, the data for the first 90 s were discarded. Measurements were taken every 30 min. Data were recorded with a data logger (CR1000; Campbell Scientific, USA). The closed chamber flux measurement was accepted if the determination coefficient of linear regression (R²) was larger than 0.85 according to the previous reports [11,41].

R_s was calculated from the rate of increase in CO₂ concentration with time using the following linear regression:

$$R_s = \frac{dc}{dt} \times \frac{V}{A} \times \rho_{airmol} \quad (\text{Eq 1})$$

where dc/dt is the rate of increase in the gas concentration c (ppm) with time t (s) and is determined by the linear least-squares method on the slope of the change in gas concentration from 90 to 180 s at the start of measurement; V is the chamber volume (0.018 m³); A is the soil surface area in the chamber (0.09 m²); and ρ_{airmol} is the air molar density (mol m⁻³).

For soil environmental monitoring, soil temperatures at 2-cm depth were measured using copper-constantan thermocouples. Soil moisture levels at 0–30 cm depth were determined with three water content reflectometers (CS615 or CS616; Campbell Scientific, USA). Data were logged continuously at each plot at 30-min intervals. Precipitation was measured with a tipping-bucket rain gauge at an open screen site near the flux tower.

For evaluating GPP, the fluxes of CO₂ (μmol m⁻² s⁻¹) were measured by open-path eddy covariance methods at a tower height of 28.5 m with a CO₂/H₂O gas analyzer (LI-7500; Li-cor, Inc., Lincoln, NE, USA). from January 2005 to December 2010. The study by Kosugi et al. [40] provides detailed information regarding the eddy covariance flux observations and calculations.

Soil respiration models

To estimate the best fit of soil temperature control on R_s rates, two empirical models, i.e., the simple exponential function model and the Arrhenius equation model, were tested. Because of the complexity of the soil environment, many researchers depend on empirical models instead of process-based models to estimate soil respiration [7]. The simplest model is the exponential increase in respiration rate as a function of temperature. The model and its parameter space are defined as

$$R_s = R_{s,ref} \times Q_{10}^{\frac{T_{soil}-T_{ref}}{10}} \quad (\text{Eq 2; Q10model})$$

where $R_{s,ref} > 0$ and $a1 > 0$. R_s and $R_{s,ref}$ are the respiration rates (μmol m⁻² s⁻¹) at

temperatures T_{soil} and T_{ref} , respectively. T_{soil} is the observed soil temperature and $T_{\text{ref}} = 15^\circ\text{C}$. Q_{10} is the temperature sensitivity and represents the relative increase in respiration as the temperature rises by 10°C . Eq 2 is often called the Q_{10} model.

The second model is the Arrhenius equation. It is also used to describe temperature dependence of respiration [44]. Since respiration increases with temperature, this model and its parameter space are defined as

$$R_s = R_{s,\text{ref}} e^{\frac{-E_a}{R \times T_{\text{soil}}}} \quad (\text{Eq 3; Arrheniusmodel})$$

where E_a is a free parameter analog to the activation energy in the standard Arrhenius model and represents the sensitivity of R_s to temperature. R is the gas constant ($R = 8.314 \text{ J K}^{-1} \text{ mol}^{-1}$). Eq 3 (the Arrhenius model) can predict the behavior of chemical systems according to enzyme kinetics that describe the relationships between enzyme activity and temperature.

Data analysis

To remove outliers, residual analyses were performed. Data points of R_s were removed from the regression when the residual of an individual data point was greater than three times the standard deviation. R_s was calculated as the mean of the three chambers and was used in subsequent analyses. Instrument failure and quality control procedures reduced the data by 10% during the 6 years of observation. We evaluated the empirical models of soil respiration at each soil temperature for the years from 2005 to 2010. Two commonly used models (Eqs 2 and 3), both of which fit the data well, were used to analyze the response of R_s to soil temperature. The Akaike information criterion (AIC) and the root mean squared error (RMSE) were used to evaluate the goodness of fit for the R_s models. The observed R_s and predicted R_s by the best-fit R_s -temperature model were calculated to determine the direction and magnitude of the seasonal dependence of R_s measurements beyond temperature-response property. To better characterize seasonal Q_{10} and E_a , monthly mean values were calculated for the years from 2005 to 2010.

The mean diurnal cycles of R_s and GPP for each month were determined by calculating the average of the 30-min data at each time of day. The cycles were then used to identify the relationship between R_s and soil temperature.

Results

Soil environmental factors and carbon exchange over six years

The mean soil water content at 0–30 cm depth ranged from 0.05 to $0.24 \text{ m}^3 \text{ m}^{-3}$ of soil (Fig 1A). Seasonal soil temperature patterns were observed (Fig 1B). The mean soil temperature at 2 cm depth varied seasonally, ranging from 0°C in February to 25°C in August during the years from 2005 to 2010. The half-hourly R_s rates measured with the automated chamber ranged from 0.1 to $10.9 \mu\text{mol m}^{-2} \text{ s}^{-1}$ during the years from 2005 to 2010 (Fig 1C). R_s showed strong seasonality; it was the lowest in February and the highest in mid-August. Seasonal variations in daily GPP over the course of this study are illustrated in Fig 1D.

Seasonal variation of soil respiration in relation to temperature and gross primary production

Two models of the correlation between R_s and soil temperature were tested to obtain the best-fit curves. RMSE and AIC based on the R_s -soil temperature relationship were smaller in the Arrhenius model than in the Q_{10} model (Table 1). When pooling data of all seasons, the Q_{10} and E_a value was 2.42 and $61.69 \text{ kJ mol}^{-1}$, respectively. A better fit for the Arrhenius model

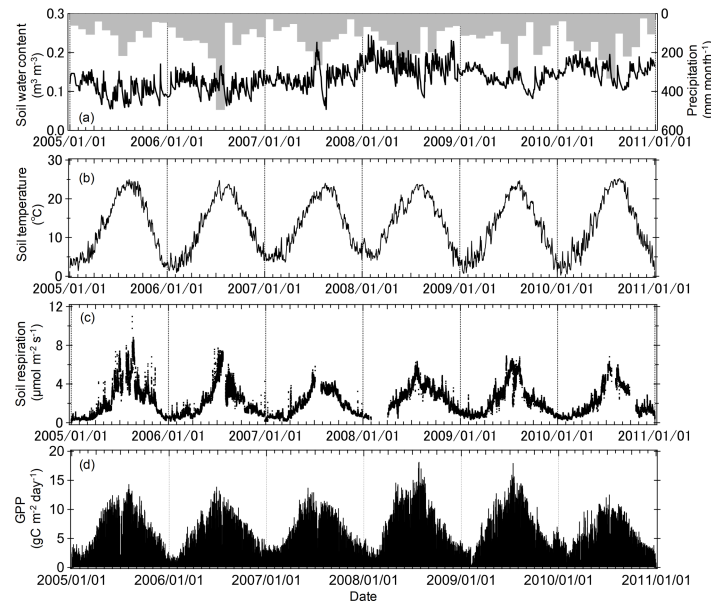


Fig 1. Time courses of (a) mean soil water content at 0–30 cm depth ($n = 3$) and precipitation levels, (b) mean soil temperature at 2 cm depth ($n = 3$), (c) half-hourly mean soil respiration rates ($n = 3$), (d) gross primary production (GPP) according to eddy covariance tower observations during the years from 2005 to 2010.

<https://doi.org/10.1371/journal.pone.0192622.g001>

was found for the relationship of R_s with soil temperature for the years from 2005 to 2010 and was used in further analyses.

In all seasons, R_s exponentially increased with soil temperature (Fig 2). The Arrhenius model explained a significant portion of the variation in R_s in response to soil temperature (Table 1). Monthly mean values of observed R_s were the highest in July and the lowest in February. In contrast, the monthly predicted R_s were the highest in August and the lowest in February. The underestimations of the predicted- to observed R_s were found for June–July. In contrast, the overestimations were observed for January–May and August–September.

There was a seasonal relationship between GPP and R_s of an evergreen conifer (Fig 3). We observed greater R_s relative to GPP in autumn for September to November when compared with spring for March to May.

Seasonal patterns in Q_{10} and E_a values

The Q_{10} and E_a values of the monthly R_s were 1.09–2.43 and 5.61–56.89 kJ mol^{-1} , respectively (Table 2). Changes in Q_{10} and E_a values were related to seasonal patterns; the values were higher in winter than in summer. For all collected samples, the Q_{10} and E_a values of R_s declined markedly with increasing soil temperature, according to the seasons, which explained a significant proportion of the variation in the temperature sensitivity of R_s ($r = 0.88, p < 0.001$; Fig 4A, $r = 0.83, p < 0.001$; Fig 4B).

Table 1. Empirical equations and parameter estimates describing the relationship between soil respiration and temperature from 2005 to 2010 ($n = 94904$). The Akaike information criterion (AIC) and the root mean squared error (RMSE) are used to evaluate the best fit for the models.

Model	Equation and parameter estimates	RMSE	AIC
Q_{10} model	$R_s = R_{s_{ref}} \times Q_{10}^{\frac{T_{soil} - T_{ref}}{10}} = 0.57 \times 2.42^{\frac{T_{soil} - 15}{10}}$	0.68	196173
Arrhenius model	$R_s = R_{s_{ref}} e^{\frac{-E_a}{R \times T_{soil}}} = 2.18 e^{\frac{-61092}{8.31 \times T_{soil}}}$	0.67	194786

<https://doi.org/10.1371/journal.pone.0192622.t001>

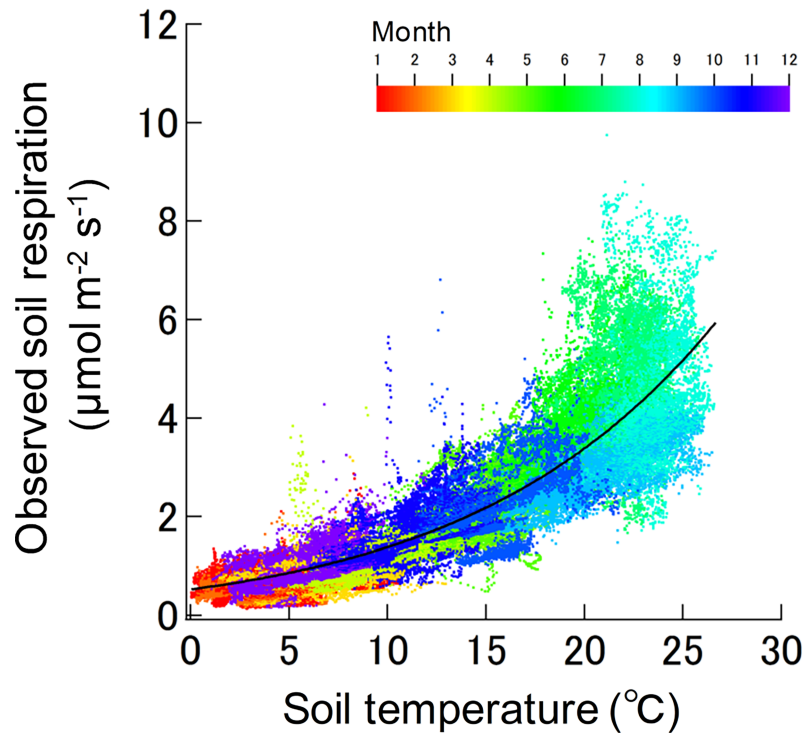


Fig 2. Relationship between soil respiration and temperature during 2005–2010 as determined by the automated chamber system. The best-fit linear relationship from the Arrhenius model is shown by the solid black line (Table 1). The rainbow color scale shows the month when the data were obtained.

<https://doi.org/10.1371/journal.pone.0192622.g002>

Diurnal variation in soil respiration with seasons

Fig 5 shows the monthly time course of R_s and GPP. On a diurnal scale, R_s rates were frequently higher from 1200 to 1800 h, decreasing overnight and reaching their minimum values in the early morning. GPP was highest at 1100–1300h and decreased slightly during the afternoon. There was a lag between the time when maximum GPP and maximum R_s were reached.

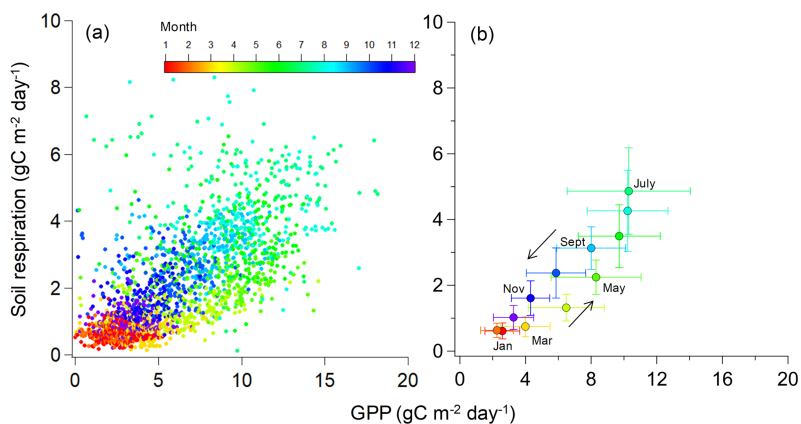


Fig 3. Relationship between daily soil respiration and gross primary production (GPP) during 2005–2010. (a) Each point represents an individual daily observation. (b) Each point is a mean value (\pm SD) for samples within a month. Color distributions were convergent in the monthly data.

<https://doi.org/10.1371/journal.pone.0192622.g003>

Table 2. Mean soil temperature, Q_{10} , and activation energy (E_a) for each month during 2005–2010.

Month	Soil temperature ° C	Q_{10}	E_a kJ mol ⁻¹
1	3.90	3.90	56885
2	4.16	2.08	50937
3	5.73	1.91	52017
4	10.21	2.55	37197
5	14.78	2.96	39873
6	18.44	3.07	34177
7	21.95	3.14	14599
8	23.15	2.89	5613
9	20.74	2.30	28634
10	15.62	1.56	49293
11	10.41	0.95	37084
12	5.75	0.48	40521

<https://doi.org/10.1371/journal.pone.0192622.t002>

A relationship between diurnal R_s and soil temperature was observed for each month, and a strong seasonal fluctuation in the relationship was also observed (Fig 6). For example, the diurnal pattern of R_s rates during July and August differed from that in other seasons. In August after the morning peaks, the R_s rates decreased around noon but soil temperatures remained high. R_s recovered in the afternoon, lagging behind the peak in soil temperature and resulting in a figure-eight curve (Fig 6H). In September and October, R_s relative to the temperature was higher in the morning than in the night, despite nearly constant soil temperatures (Fig 6I and 6J). Therefore, diurnal R_s rates showed a hysteresis pattern in seasons with high biological activity (Fig 6). In contrast, the R_s rates in seasons where biological activity ceases changed exponentially and showed negligible hysteresis.

Discussion

From six years of observation by automated chambers, we characterised the magnitude and pattern of seasonal and diurnal R_s in an evergreen coniferous forest. This information may enable more accurate prediction of soil C dynamics and their associated ecosystem processes.

Our results support the hypothesis that high-frequency observations of R_s rates clearly indicate the seasonal changes in the response of R_s to soil temperature in field conditions, so that soil temperature alone is clearly insufficient to predict R_s . In this study, R_s increased exponentially with increasing soil temperature. This correlation explained 80% of the variation in R_s across seasons when the best-fit Arrhenius model was used. In addition, the temperature sensitivity in this study was consistent with the findings of previous studies [45]. Our Q_{10} values were well within the global median of 2.4 [46] and the range (2.0–6.3) reported for European and North American forest ecosystems [47,48]. The Arrhenius function reveals the reactions with E_a around 50 kJ mol⁻¹ [7], in agreement with our field observations. Nevertheless, there was a strong seasonal fluctuation in the relationship between R_s and soil temperature. The predicted R_s underestimated the actual R_s for June and July and overestimated R_s for August and September (Fig 2). Our results corroborate those of previous studies that reported increases in the contributions of R_s to ecosystem respiration during early summer [14,49]. This is probably due to the compensation of the model bias in late summer and autumn (overestimation) and early summer (underestimation), without explicit dependence of R_s on phenological attributes.

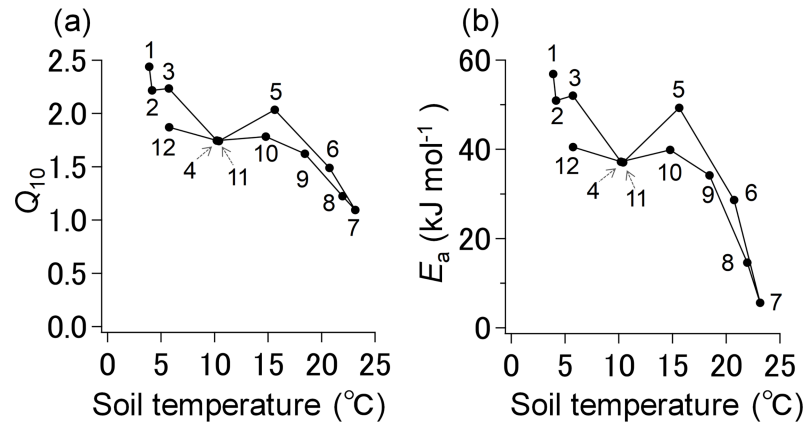


Fig 4. Relationship between (a) Q_{10} and (b) activation energy (E_a) of soil respiration and temperature for each month. Numbers in the figure indicate months.

<https://doi.org/10.1371/journal.pone.0192622.g004>

We found that there was a hysteresis in the seasonal relationship between GPP and R_s of an evergreen conifer (Fig 3). Seasonal patterns in R_s rates may be due to root production and respiration levels. Endogenous and phenological C assimilation rates are strongly correlated with belowground C allocation to roots, mycorrhizae, and rhizosphere microorganisms [28,29,50,51]. Root growth is assumed to peak early in the growing season and is therefore correlated with aboveground growth [52]. When a pulse of root growth occurs to support leaf production, the amount of respiring tissue and root CO₂ emission simultaneously increase. In this study site, GPP relative to the solar radiation and temperature was higher during the spring and summer [40]. Kosugi et al. [40] noted that red leaf pigmentation in the winter prevented light inhibition at low temperatures and affected stomatal conductance and photosynthetic rates in an evergreen coniferous forest. Substrate limitation in the rhizosphere during the winter may reduce root growth and autotrophic respiration rates. Therefore, seasonal

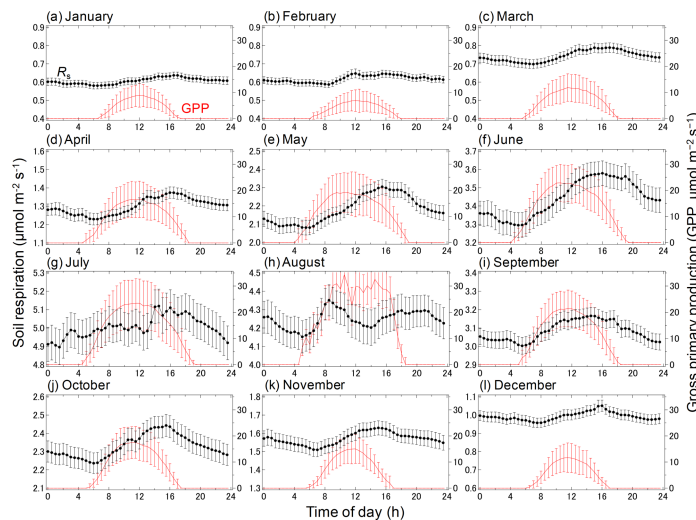


Fig 5. Diurnal variations in soil respiration and gross primary production (GPP) for each month. Error bars represent the standard errors of the mean for each month from 2005 to 2010. Each figure shows the fixed-width from bottom to top in Y-axis in all months.

<https://doi.org/10.1371/journal.pone.0192622.g005>

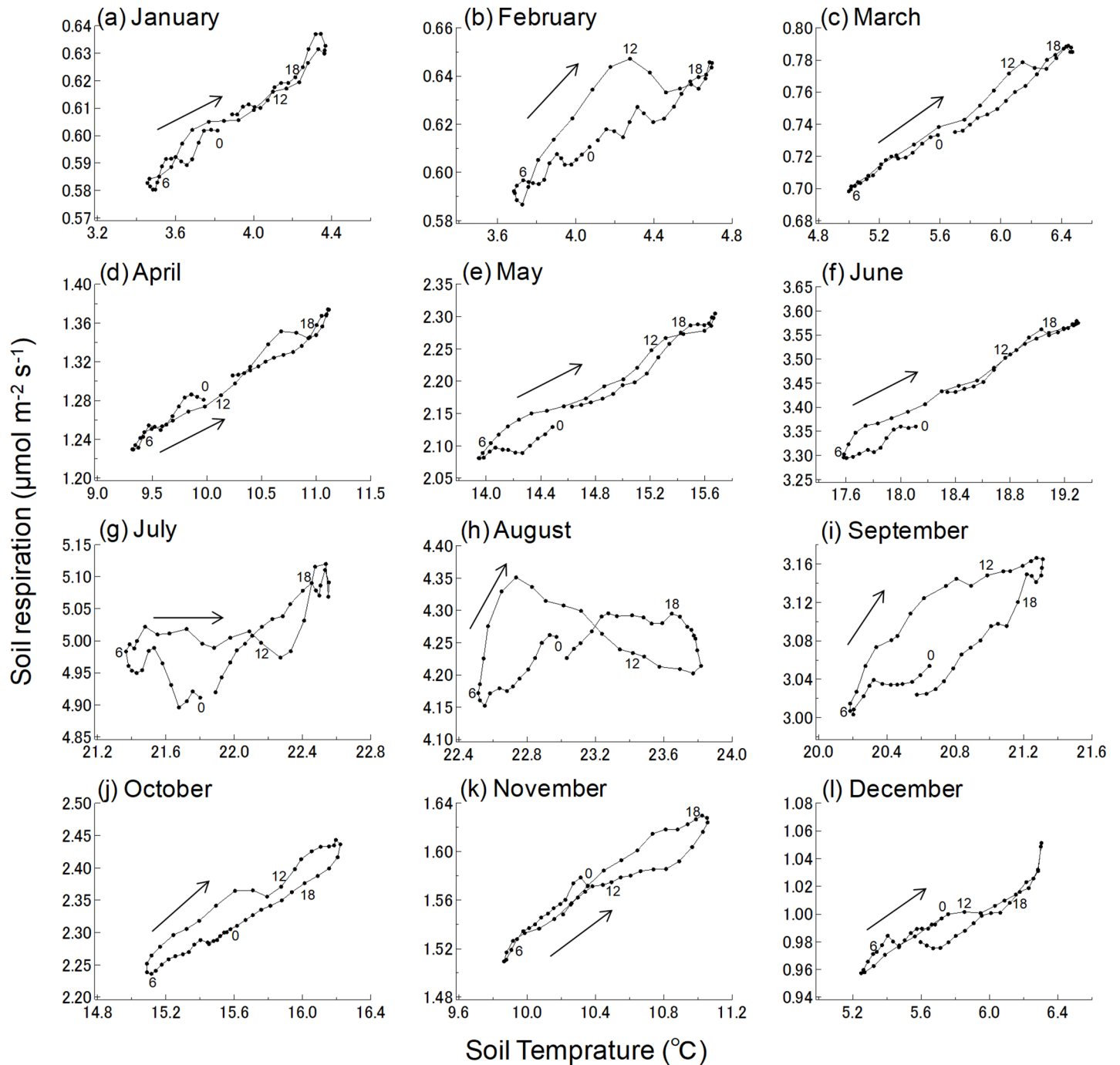


Fig 6. Relationship between soil respiration and temperature for each month. Each point indicates the mean value. Numbers in the figure indicate time of day of the mean for each month from 2005–2010.

<https://doi.org/10.1371/journal.pone.0192622.g006>

plant phenology patterns may lead to variation in the substrate supply and belowground C allocation, and partly affect variation in R_s [39].

The level of heterotrophic respiration is also indicative of the seasonal patterns of R_s , particularly for the decline in observed R_s rates during August and September. In Asian monsoon areas, microbial decomposition is often enhanced during the early summer rainy season and

suppressed by the late summer drought conditions [53]. Heterotrophic respiration is sensitive to seasonal rainfall patterns because soil water content strongly affects microbial physiology [12]. The biodiversity and metabolic activity of most soil microbial communities decrease with soil water content [54,55]. In fact, we found a significantly negative relationship between the temperature sensitivity of R_s and temperature; monthly Q_{10} and E_a were highest in winter and lowest in summer (Fig 4). These seasonal patterns in temperature sensitivity may be related to degradation of soil C, microbial physiological acclimation and community adjustment [55,56] by changing their lipid composition, synthesizing new proteins, and changing resource allocation from growth to survival mechanisms [57,58]. Previous studies reported that heterotrophic respiration and nutrient mineralization under drought also declined [58–60]. Consequently, the decline in R_s during the late summer is mostly related to a changed temperature response due to changed sensitivity of microbial degradation to water stress.

However, the seasonal R_s pattern in the present study contrasts with those reported previously [61]. Lee et al. [62] showed that R_s in a cool-temperate Japanese deciduous broad-leaved forest was lower in spring and early summer than in late summer and autumn. This difference may be explained by seasonal changes in soil heat transport and CO_2 fluxes [34,63]. In spring, when soils are covered with snow, the contributions of root and microbial activity are reduced by the low temperatures in deeper soil layers, but the opposite occurs in late summer and autumn. In late summer, the R_s components increase in response to the warming of the deeper soil layers. Soils usually warm from the top downward in spring and cool from the top downward in autumn. The presence of snow and the timing of early spring thaw and late autumn frost affect the vertical distribution of soil temperature. In addition, high R_s in a deciduous forest in autumn could also be related to the high input of litter during autumn. Therefore, variation in CO_2 production with soil depth during the growing season may affect heat transport-based hysteresis.

The coordination of aboveground and belowground phenological patterns would contribute to the seasonality of the R_s diurnal scale hysteresis. In September and October, R_s relative to the soil temperature was higher in the morning than at night. Diurnal hysteresis in the relationship between R_s and soil temperature is an example of multiple processes interacting to produce highly variable photosynthetic attributes [30,31]. Liu et al. [17] showed that the diurnal cycle of R_s in a mixed deciduous forest was related more to differences in photosynthetically active radiation than to variations in soil environmental conditions, suggesting that diurnal R_s patterns were associated with photosynthesis. In the present study, diurnal R_s was higher in the morning than in the nighttime, especially in September and October. The diurnal R_s pattern of the relationship between R_s and soil temperature showed a hysteresis loop. The R_s morning peaks in September and October suggest faster transfer of recent photosynthates to belowground in warm-temperate ecosystems. In fact, the R_s peaks occurred later than GPP peaks (Fig 5I and 5). Our results suggest that soil temperature does not fully explain variations in diurnal R_s dynamics.

Interestingly, figure-eight-shaped diurnal R_s patterns were observed in July and August (Fig 6). This finding suggests that midday declines in root physiological activity may have occurred in early summer. Under natural field conditions, plants adapt to changes in the prevailing irradiance to protect and optimize photosynthesis. As a result, continuous daily variations occur. Photooxidative damage to leaf thylakoid membranes causes photoinhibition and stomatal closure. The leaf protects the photosynthetic apparatus by down-regulating it at higher temperatures under high photon flux [64]. Photoinhibitory damage and stomatal closure contribute significantly to midday photosynthetic depression and, indirectly, to the decline in C supply to the root system. Makita et al. [31] showed that weather conditions under high temperature stress cause a midday depression of CO_2 assimilation in deciduous trees and then a sharp

reduction in autotrophic respiration rate. The flux of new photosynthate to the rhizosphere significantly accelerates microbial activity there. This process affects the relative amount of heterotrophic respiration from decomposition of soil organic matter [33,65]. The results of the present study indicate how canopy processes affect the phase lags between the diurnal signals of soil temperature and forest floor R_s . Some studies have suggested that the autotrophic component of R_s is controlled by carbohydrate production and internal transport in trees more than by diurnal variations in environmental variables [13,30]. Therefore, diurnal variation in R_s may explain the hysteresis loop observed in this study. Nevertheless, there remains some debate over the relative importance of temperature- and substrate-dependent processes as drivers of midday photosynthesis depression in actual R_s rates. There is little evidence that root growth and other C sinks are determined by substrate availability [66]. The associations between photosynthesis and R_s may be controlled by multiple factors, including photosynthate transport distance, root depth, plant physiology, growth stage, and environmental conditions [15,67]. Recent advances in isotopic labeling techniques have enabled the quantification of C partitioning in forests and the assessment of its role in tree growth, resource acquisition, and C sequestration at temporal scales [37,38]. Further investigation is needed to establish the mechanisms of aboveground–belowground interactions and the factors that control them.

In conclusion, continuous monitoring of R_s rates in a warm-temperate evergreen coniferous forest with an automated chamber system demonstrated diverse biological phases of the R_s rate at different time scales independently of soil temperature. We found that the magnitude and pattern of temporal R_s was depend on seasons across the temperature dependence. Additionally, more research is needed to elucidate whether the impact of linkage between aboveground and belowground C allocation depends on vegetation types and features of the soil environment, such as moisture. Soil CO₂ efflux data with a high temporal resolution would help to quantify the contributions of abiotic and biotic effects on C flux and sequestration in forest soils.

Supporting information

S1 Fig. Mean monthly air temperature (°C) precipitation (mm) for the period 2005–2010. Error bars represent standard deviations. Data were from Y. Kosugi et al. [40]. (TIF)

Acknowledgments

The authors acknowledge the laboratory members of the forest hydrology at Kyoto University for supports in field and laboratory experiments.

Author Contributions

Conceptualization: Naoki Makita, Yoshiko Kosugi, Ayaka Sakabe.

Data curation: Naoki Makita, Yoshiko Kosugi, Akito Kanazawa, Shinjiro Ohkubo.

Formal analysis: Naoki Makita.

Funding acquisition: Yoshiko Kosugi, Makoto Tani.

Investigation: Naoki Makita.

Methodology: Naoki Makita, Ayaka Sakabe, Shinjiro Ohkubo.

Project administration: Naoki Makita.

Resources: Naoki Makita.

Software: Naoki Makita.

Supervision: Naoki Makita.

Validation: Naoki Makita.

Visualization: Naoki Makita.

Writing – original draft: Naoki Makita, Yoshiko Kosugi, Ayaka Sakabe.

Writing – review & editing: Naoki Makita, Akito Kanazawa, Makoto Tani.

References

1. Scharlemann JP, Tanner EV, Hiederer R, Kapos V. Global soil carbon: understanding and managing the largest terrestrial carbon pool. *Carbon Manag.* 2014; 5: 81–91.
2. Bond-Lamberty B, Thomson A. Temperature-associated increases in the global soil respiration record. *Nature.* 2010; 464:579–582 <https://doi.org/10.1038/nature08930> PMID: 20336143
3. Ryan MG, Law BE. Interpreting, measuring, and modeling soil respiration. *Biogeochemistry.* 2005; 73: 3–27
4. Heimann M, Reichstein M. Terrestrial ecosystem carbon dynamics and climate feedbacks. *Nature.* 2008; 451:289–292 <https://doi.org/10.1038/nature06591> PMID: 18202646
5. Bond-Lamberty B, Wang C, Gower ST. A global relationship between the heterotrophic and autotrophic components of soil respiration? *Glob Change Biol.* 2004; 10:1756–1766
6. Pumpanen J, Longdoz B, Kutsch WL. Field measurements of soil respiration: principles and constraints, potentials and limitations of different methods. In: Kutsch W.L., Bahn M., Heinemeyer A.(Eds.). *Soil Carbon Dynamics—An Integrated Methodology.* 2009; pp. 16–33. Cambridge University Press.
7. Davidson E, Janssens IJ, Luo Y. On the variability of respiration in terrestrial ecosystems: moving beyond Q_{10} . *Glob Change Biol.* 2006; 12: 154–164.
8. Riveros-Iregui DA, Emanuel RE, Muth DJ, McGlynn BL, Epstein HE, Welsch DL et al. Diurnal hysteresis between soil CO₂ and soil temperature is controlled by soil water content. *Geophys Res Lett.* 2007; 34: L17404
9. Carbone MS, Vargas R. Automated soil respiration measurements: new information, opportunities and challenges. *New Phytol.* 2008; 177:295–297
10. Pumpanen J, Kolari P, Ilvesniemi H, Minkkinen K, Vesala T, Niinisto S et al. Comparison of different chamber techniques for measuring soil CO₂ efflux. *Agric For Meteorol.* 2004; 123:159–176
11. Savage K, Davidson EA, Richardson AD. A conceptual and practical approach to data quality and analysis procedures for high-frequency soil respiration measurements. *Funct Ecol.* 2008; 22:1000–1007
12. Xu L, Baldocchi DD, Tang J. How soil moisture, rain pulses, and growth alter the response of ecosystem respiration to temperature. *Global Biogeochemical Cycles.* 2004; 18: GB4002
13. Tang J, Baldocchi DD, Xu L. Tree photosynthesis modulates soil respiration on a diurnal time scale. *Glob Change Biol.* 2005; 11:1298–1304
14. Gaumont-Guay D, Black TA, Barr AG, Jassal RS, Nesic Z. Biophysical controls on rhizospheric and heterotrophic components of soil respiration in a boreal black spruce stand. *Tree Physiol.* 2008; 28:161–171. PMID: 18055427
15. Kuzyakov Y, Gavrichkova O. Time lag between photosynthesis and CO₂ efflux from soil: A review of mechanisms and controls. *Glob Change Biol.* 2010; 16:3386–3406.
16. Bloemen J, Agneessens L, Van Meulebroek L, Aubrey DP, McGuire MA, Teskey RO et al. Stem girdling affects the quantity of CO₂ transported in xylem as well as CO₂ efflux from soil. *New Phytol.* 2014; 201:897–907 <https://doi.org/10.1111/nph.12568> PMID: 24400900
17. Liu Q, Edwards NT, Post WM, Gu L, Ledford J, Lenhart S. Temperature-independent diel variation in soil respiration observed from a temperate deciduous forest. *Glob Change Biol.* 2006; 12: 2136–2145.
18. Curiel-Yuste J, Janssens IA, Carrara A, Meiresonne L, Ceulemans R. Interactive effect of temperature and precipitation on soil respiration in a temperate maritime pine forest. *Tree Physiol.* 2003; 23:1263–1270. PMID: 14652226
19. Bahn M, Reichstein M, Davidson EA, Grünzweig J, Jung M, Carbone MS et al. Soil respiration at mean annual temperature predicts annual total across vegetation types and biomes. *Biogeosciences.* 2010; 7: 2147–2157. <https://doi.org/10.5194/bg-7-2147-2010> PMID: 23293656

20. Menzel A, Sparks-Tim H, Estrella N, Koch E, Aasa A, Ahas R et al. European phenological response to climate change matches the warming pattern. *Glob Change Biol.* 2006; 12: 1969–1976.
21. Baldocchi D. Breathing of the terrestrial biosphere: lessons learned from a global network of carbon dioxide flux measurement systems. *Australian Journal of Botany.* 2008; 56: 1–26.
22. Heskell MA, Atkin OK, Turnbull MH, Griffin KL. Bringing the Kok effect to light: a review on the integration of daytime respiration and net ecosystem exchange. *Ecosphere.* 2013; 4: art98
23. McCormack ML, Adams TS, Smithwick EAH, Eissenstat DM. Predicting fine root lifespan from plant functional traits in temperate trees. *New Phytol.* 2012; 195:823–831. <https://doi.org/10.1111/j.1469-8137.2012.04198.x> PMID: 22686426
24. Tierney GL, Fahey TJ, Groffman PM, Hardy JP, Fitzhugh RD, Driscoll CT et al. Environmental control of fine root dynamics in a northern hardwood forest. *Glob Change Biol.* 2003; 9: 670–679
25. Steinaker DF, Wilson SD, Peltzer DA. Asynchronicity in root and shoot phenology in grasses and woody plants. *Glob Change Biol.* 2010; 16: 2241–2251.
26. Höglberg P, Read DJ. Towards a more plant physiological perspective on soil ecology. *Trends Ecol Evol.* 2006; 21:548–554 <https://doi.org/10.1016/j.tree.2006.06.004> PMID: 16806577
27. Jones DL, Nguyen C, Finlay RD. Carbon flow in the rhizosphere: carbon trading at the soil-root interface. *Plant Soil.* 2009; 321: 5–33.
28. Heinemeyer A, Wilkinson M, Vargas R, Subke JA, Casella E, Morison JIL et al. Exploring the “overflow tap” theory: linking forest soil CO₂ fluxes and individual mycorrhizosphere components to photosynthesis. *Biogeosciences.* 2012; 9:79–95.
29. Vargas R, Baldocchi DD, Allen MF, Bahn M, Black TA, Collins SL et al. Looking deeper into the soil: biophysical controls and seasonal lags of soil CO₂ production and efflux. *Ecol Appl.* 2010; 20:1569–1582 PMID: 20945760
30. Han G, Luo Y, Li D, Xia J, Xing Q, Yu J. Ecosystem photosynthesis regulates soil respiration on a diurnal scale with a short-term time lag in a coastal wetland. *Soil Biol Biochem.* 2014; 68:85–94.
31. Makita N, Kosugi Y, Kamakura M. Linkages between diurnal patterns of root respiration and leaf photosynthesis in *Quercus crispula* and *Fagus crenata* seedlings. *Journal of Agricultural Meteorology.* 2014; 70: 151–162.
32. Keane JB, Ineson P. Differences in the diurnal pattern of soil respiration under adjacent *Miscanthus giganteus* and barley crops reveal potential flaws in accepted sampling strategies. *Biogeosciences.* 2017; 14:1181–1187.
33. Bhupinderpal-Singh, Nordgren A, Ottosson-Löfvenius M, Höglberg MN, Mellander PE, Höglberg P. Tree root and soil heterotrophic respiration as revealed by girdling of boreal Scots pine forest: extending observations beyond the first year. *Plant Cell Environ.* 2003; 26: 1287–1296
34. Phillips CL, Nickerson N, Risk D, Bond BJ. Interpreting diel hysteresis between soil respiration and temperature. *Glob Change Biol.* 2011; 17: 515–527.
35. Bahn M, Schmitt M, Siegwolf R, Richter A, Brüggemann N. Does photosynthesis affect grassland soil-respired CO₂ and its carbon isotope composition on a diurnal timescale? *New Phytol.* 2009; 182:451–460 <https://doi.org/10.1111/j.1469-8137.2008.02755.x> PMID: 19220762
36. Ruehr NK, Knohl A, Buchmann N. Environmental variables controlling soil respiration on diurnal, seasonal and annual time-scales in a mixed mountain forest in Switzerland. *Biogeochemistry.* 2010; 98:153–170
37. Dannoura M, Maillard P, Fresneau C, Plain C, Berveiller D, Gerant D et al. In situ assessment of the velocity of carbon transfer by tracing ¹³C in trunk CO₂ efflux after pulse labelling: variations among tree species and seasons. *New Phytol.* 2011; 190: 181–192. <https://doi.org/10.1111/j.1469-8137.2010.03599.x> PMID: 21231935
38. Epron D, Bahn M, Derrien D, Lattanzi FA, Pompanen J, Gessler A et al. Pulse-labelling trees to study carbon allocation dynamics: a review of methods, current knowledge and future prospects. *Tree Physiol.* 2012; 32: 776–798. <https://doi.org/10.1093/treephys/tps057> PMID: 22700544
39. DeForest JL, Noormets A, McNulty SG, Sun G, Tenney G, Chen JQ. Phenophases alter the soil respiration–temperature relationship in an oak-dominated forest. *Int J Biometeorol.* 2006; 51:135–144. <https://doi.org/10.1007/s00484-006-0046-7> PMID: 16874506
40. Kosugi Y, Takanashi S, Ueyama M, Ohkubo S, Tanaka H, Matsumoto K et al. Determination of the gas exchange phenology in an evergreen coniferous forest from 7 years of eddy covariance flux data using an extended big-leaf analysis. *Ecol Res.* 2013; 28: 373–385
41. Sakabe A, Kosugi Y, Takahashi K, Kanazawa A, Itoh M, Makita N et al. One year of continuous measurements of soil CH₄ and CO₂ fluxes in a Japanese cypress forest: temporal and spatial variations associated with Asian monsoon rainfall. *J Geophys Res–Biogeosciences.* 2015; 120: 585–599

42. Ohkubo S, Kosugi Y, Takanashi S, Mitani T, Tani M. Comparison of the eddy covariance and automated closed chamber methods for evaluating nocturnal CO₂ exchange in a Japanese cypress forest. *Agric For Meteorol.* 2007; 142: 50–65.
43. Mitani T, Kosugi Y, Osaka K, Okubo S, Takanashi S, Tani M. Spatial and temporal variability of soil respiration rate at a small watershed revegetated with Japanese Cypress. *J Jpn For Soc.* 2006; 88: 496–507.
44. Lloyd J, Taylor JA. On the temperature dependence of soil respiration. *Funct Ecol.* 1994; 8:315–323
45. Hamdi S, Moyano F, Sall S, Bernoux M, Chevallier T. Synthesis analysis of the temperature sensitivity of soil respiration from laboratory studies in relation to incubation methods and soil conditions. *Soil Biol Biochem.* 2013; 58:115–126.
46. Raich JW, Schlesinger WH. The global carbon dioxide flux in soil respiration and its relationship to vegetation and climate. *Tellus.* 1992; 44B:81–99.
47. Davidson EA, Belk E, Boone RD. Soil water content and temperature as independent or confounded factors controlling soil respiration in a temperate mixed hardwood forest. *Glob Change Biol.* 1998; 4:217–227.
48. Janssens IA, Pilegaard K. Large seasonal changes in Q₁₀ of soil respiration in a beech forest. *Glob Change Biol.* 2003; 9:911–918.
49. Irvine J, Law BE, Martin JG, Vickers D. Interannual variation in soil CO₂ efflux and the response of root respiration to climate and canopy gas exchange in mature ponderosa pine. *Glob Change Biol.* 2008; 14:2848–2859.
50. Joslin JD, Wolfe MH, Hanson PJ. Factors controlling the timing of root elongation intensity in a mature upland oak stand. *Plant Soil.* 2001; 228:201–212.
51. Curiel-Yuste J, Janssens IA, Carrara A, Ceulemans R. Annual Q₁₀ of soil respiration reflects plant phenological patterns as well as temperature sensitivity. *Glob Change Biol.* 2004; 10: 161–169.
52. Medvigy D, Wofsy SC, Munger JW, Hollinger DY, Moorcroft PR. Mechanistic scaling of ecosystem function and dynamics in space and time: EcosystemDemography model version 2. *Journal of Geophysical Research.* 2009; 114: G01002.
53. Cook ER, Anchukaitis KJ, Buckley BM, D'Arrigo RD, Jacoby GC, Wright WE. Asian monsoon failure and megadrought during the last millennium. *Science.* 2010; 328:486–489 <https://doi.org/10.1126/science.1185188> PMID: 20413498
54. Kawamura A, Makita N, Osawa A. Response of microbial respiration from fine root litter decomposition to root water content in a temperate broadleaved forest. *Plant Root.* 2013; 7:77–82.
55. Conant RT, Ryan MG, Ågren GI, Birge HE, Davidson EA, Eliasson PE et al. Temperature and soil organic matter decomposition rates—synthesis of current knowledge and a way forward. *Glob Chang Biol.* 2011; 17:3392–3404.
56. Makita N, Kawamura A. Temperature sensitivity of microbial respiration of fine root litter in a temperate broad-leaved forest. *PLoS One.* 2015; 10:e0117694 <https://doi.org/10.1371/journal.pone.0117694> PMID: 25658106
57. Suzina NE, Mulyukin AL, Kozlova AN, Shorokhova AP, Dmitriev VV, Barinova ES et al. Ultrastructure of resting cells of some non-spore-forming bacteria. *Microbiology.* 2004; 73:435–447.
58. Schimel J, Balsler TC, Wallenstein M. Microbial stress-response physiology and its implications for ecosystem function. *Ecology.* 2007; 88:1386–1394. PMID: 17601131
59. Manzoni S, Jackson RB, Trofymow JA, Porporato A. The global stoichiometry of litter nitrogen mineralization. *Science.* 2008; 321: 684–686. <https://doi.org/10.1126/science.1159792> PMID: 18669860
60. Moyano FE, Vasilyeva N, Bouckaert L, Cook F, Craine J, Curie Yuste J et al. The moisture response of soil heterotrophic respiration: interaction with soil properties. *Biogeosciences.* 2012; 9:1173–1182.
61. Drewitt GB, Black TA, Nesic Z, Humphreys ER, Jork EM, Swanson R et al. Measuring forest-floor CO₂ fluxes in a Douglas-fir forest. *Agric For Meteorol.* 2002; 110:299–317.
62. Lee MS, Lee JS, Koizumi H. Temporal variation in CO₂ efflux from soil and snow surfaces in a Japanese cedar (*Cryptomeria japonica*) plantation, central Japan. *Ecol Res.* 2008; 23:777–785
63. Risk D, Kellman L, Beltrami H. Carbon dioxide in soil profiles: production and temperature dependence. *Geophys Res Lett.* 2002; 29:1087.
64. Franco AC, Lüttge U. Midday depression in savanna trees: coordinated adjustments in photochemical efficiency, photorespiration, CO₂ assimilation and water use efficiency. *Oecologia.* 2002; 131: 356–365. <https://doi.org/10.1007/s00442-002-0903-y> PMID: 28547707
65. Trinder CJ, Artz RRE, Johnson D. Contribution of plant photosynthate to soil respiration and dissolved organic carbon in a naturally recolonising cutover peatland. *Soil Biol Biochem.* 2008; 40:1622–1628

66. Lynch DJ, Matamala R, Iversen CM, Norby RJ, Gonzalez-Meler MA. Stored carbon partly fuels fine-root respiration but is not used for production of new fine roots. *New Phytol.* 2013; 199: 420–430. <https://doi.org/10.1111/nph.12290> PMID: [23646982](https://pubmed.ncbi.nlm.nih.gov/23646982/)
67. Abramoff RZ, Finzi AC. Are above- and below-ground phenology in sync? 2015; *New Phytol* 205:1054–1061. PMID: [25729805](https://pubmed.ncbi.nlm.nih.gov/25729805/)